

Accurate prediction of device performance in sub-10nm WFIN FinFETs using scalpel SSRM-based calibration of process simulations.

P. Eyben, P. Matagne, T. Chiarella, A. De Keersgieter, S. Kubicek, J. Mitard, A. Mocuta, N. Horiguchi, A.V-Y. Thean, D. Mocuta
Logic Technologies, IMEC Kapeldreef 75, 3001
Leuven, Belgium
E-mail: Pierre.Eyben@imec.be

Abstract— In this paper, we illustrate how high resolution two-dimensional (2D) carrier maps obtained from scalpel scanning spreading resistance microscopy (s-SSRM) can be applied to calibrate a technology computer aided design (TCAD) simulator in order to predict and understand the performance of sub-10nm WFIN FinFETs. In the proposed approach, process simulations are calibrated such that the resulting simulated carrier profiles match the quantified s-SSRM profiles. Upon reaching satisfactory agreement, they can be used as input for device simulators in order to predict more accurately key device parameters such as the linear on-state resistance ($R_{ON,LIN}$), and the threshold voltage ($V_{T,SAT}$) roll-off to name few. This also allows us to accelerate the development of devices towards new technology nodes (as N7 and N5) by identifying parameters to be improved and technological options to be selected.

Keywords—FinFET, SSRM, metrology, calibration

I. INTRODUCTION

The aggressive downscaling of FinFET devices in past years has put a great emphasis on the need to characterize two- (2D) and even three-dimensional (3D) carrier profiles for the correct understanding of device behavior. In such scaled devices even the smallest variations of the structure dimensions (ie. fin width or length, local interconnect, spacer, etc.), carrier distribution and/or activation rate can cause significant variations in the electrical properties of the devices. As physical mechanisms involved in scaled devices are complex, adequate 2D and 3D characterization techniques have been identified as a necessity by process/device engineers to achieve an accurate modeling and calibration of TCAD simulators.

To fulfill these needs, scanning spreading resistance microscopy (SSRM) has been used extensively and has demonstrated its usefulness. In essence, SSRM consists of a conductive tip mounted on an atomic force microscope (AFM) which is scanned in contact mode over the area of interest, and whereby one measures the current flowing through the sample while a DC bias is applied between the tip and a back-contact (Fig. 1). SSRM is performed at a large pressure (GPa range) which leads to a good (near ohmic) electrical contact between

the tip and the sample. The contact resistance is then dominated by the current spreading in the point contact and scales directly with the local resistivity and hence with the carrier concentration. In order to optimize the tip-sample electrical nano-contact, measurements are typically performed in a low humidity chamber (<0.1ppm H₂O and O₂). The resulting current varies over a broad dynamic range (typically 10 pA to 0.1 mA) and is measured using a logarithmic current amplifier. The successful implementation of SSRM is intimately linked to the emergence of wear resistant probes based on doped diamond. Its sub-nanometer spatial resolution combined with a doping sensitivity ranging over 5 orders of magnitude with good quantification accuracy make SSRM unique [1-4].

In this work we have utilized its most recent mode, named scalpel-SSRM (s-SSRM), wherein one is exploiting the possibility to use diamond based AFM-tips as scalpel, removing material layer by layer while scanning. s-SSRM is allowing to perform successive 2D carrier mappings [5] with a sub-2nm resolution along X-Y and Z directions. 2D carrier maps parallel to the fin in the center of sub-10nm WFIN FinFETs were generated using the s-SSRM (Fig. 2).

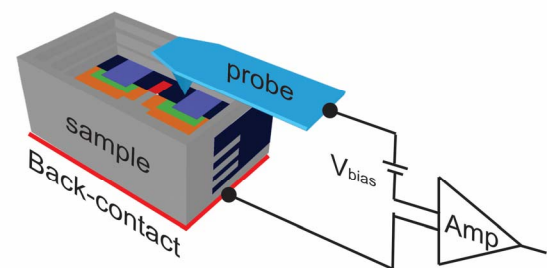


Fig. 1. 3D top-view of the scalpel-SSRM set-up. The diamond probe is utilized as a scalpel to remove material and reach the area of interest while scanning. Current (measured using a current amplifier) flowing between probe and back-contact at each position is a direct measure for the local resistivity and hence for the active dopant concentration.

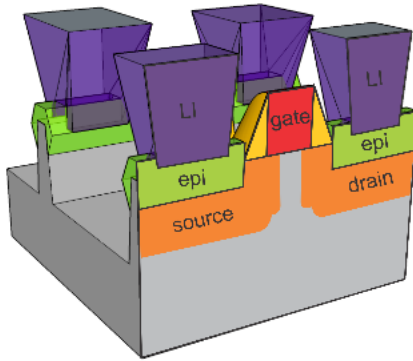


Fig. 2. Schematic representation of the 2D section in the center of the fin structure as measured with s-SSRM (see Fig. 4).

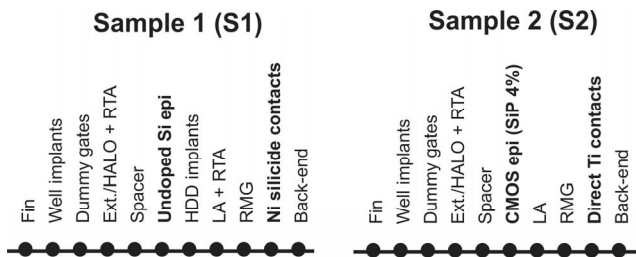


Fig. 3. Schematic processing flow of sample 1 (S1) and sample 2 (S2). Important variations (on source-drain epi and on local interconnects) are represented in bold.

II. CALIBRATION OF PROCESS SIMULATOR USING S-SSRM

A. Comparison between s-SSRM and default TCAD results

We have analyzed two different n-FinFET devices (samples S1 and S2). Key process differences (Fig. 3) between these devices are the doping procedure of recessed source-drain epi (implanted undoped Si epi in sample S1 vs. in-situ doped Si:P 4% epi in sample S2), anneals (1200°C laser anneal and 1.5s 1000°C rapid thermal annealing in S1 vs. 1100°C laser annealing in sample S2) and the local interconnect (Ni silicided contact in sample S1 vs. direct Ti contact in sample S2).

The 2D s-SSRM resistance maps (along the sub-10nm fin and in its center as illustrated in Fig.2) are presented in Fig. 4. Vertical and lateral resistance section lines (corresponding to the left-hand side scale-bar) as well as the quantified active dopant concentration section lines (right-hand side scale-bar) are presented in Fig. 5. They demonstrate a larger overlap in the case of sample S2 (12 vs. 6nm) while the extension conditions are the same for both samples.

All the process differences have been carefully included in the TCAD decks resulting in noticeable differences in the simulated carrier maps (Fig. 6). In particular, we observe in sample S2 that the extension could be covered (higher concentration and more lateral diffusion) by the carriers coming from the pre-doped source-drain epi. Difference in overlap length is confirmed by the $V_{T,SAT-LG}$ (at $V_{DS}=V_{DD}=0.8V$) exhibiting more roll-off for sample S2 (Fig. 7).

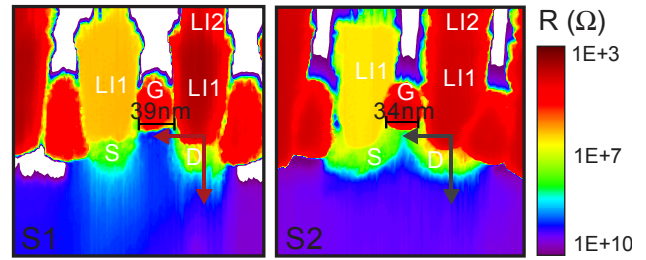


Fig. 4. 2D s-SSRM resistance maps for samples S1 and S2. Source, drain, gate and local interconnects are marked. Gate and fin lengths are measured. Arrows are highlighting vertical and lateral section lines represented in Fig. 5.

However, major differences may still be observed between these default TCAD simulations and both the s-SSRM maps and the electrical characteristics. In particular, the maximum carrier concentration (in epi and extensions) is too high in the simulations (vs. experimental s-SSRM results) and the $R_{ON,LIN}$ is too low (vs. measured values), in particular for sample S1. This is a clear indication that the process simulations are not yet properly calibrated.

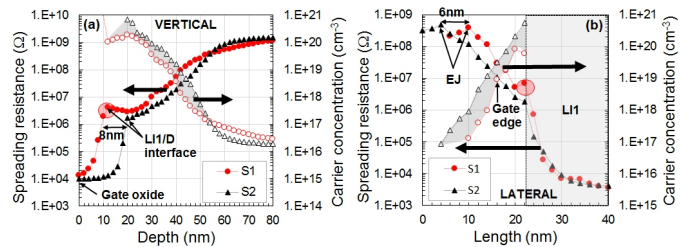


Fig. 5. Vertical spreading resistance and quantified active dopant concentration (in n-Si) section lines (aligned on gate oxide position) for samples S1 and S2. Higher active dopant concentration is highlighted for sample S2. Deeper (8nm) LI1 is also observed (a). Lateral spreading resistance and quantified active dopant concentration (in n-Si) section lines (aligned on LI1/Drain interface). Higher active dopant concentration and increased lateral diffusion (6nm) are highlighted for sample S2. A resistance peak is observed at the LI1/Drain interface for sample S1, which may impact (increase) the contact resistance (b).

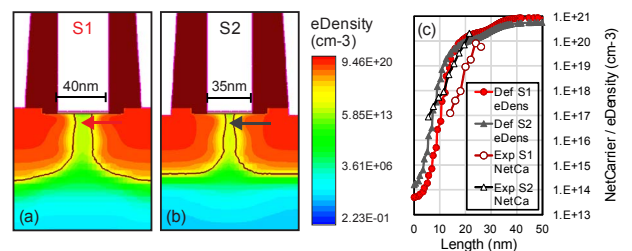


Fig. 6. 2D TCAD eDensity maps for samples S1 (a) and S2 (b). Arrows are highlighting the lateral section lines from (c). Experimental curves as extracted from s-SSRM quantified sections (and aligned to the gate edge) are superposed in (c). Poor agreement between default TCAD and s-SSRM can be observed.

B. Impact of active dose variation in extensions and source-drain

As compared to the default TCAD results, carrier (or active dopant) concentrations measured with s-SSRM (Figs. 5 and 6) exhibit lower values in the extensions (10x for sample S1 and 2x for sample S2) as well as in the source-drain epi (5-10x for sample S1 and 3x for sample S2). Hence we have investigated the impact of (active) dose loss in the extensions and variation in the source-drain epi (Table 1).

The dose loss in the extensions may originate from the resist strip step from the lithographic process performed prior to the epi growth (a softer processed is utilized for sample S2). The higher dose in the epi source-drain of sample S2 arises from the ability to incorporate very high dopant concentrations (above $1E21$ at/cm³) into in-situ doped Si:P epi.

Both dose variations are impacting the $I_{D,LIN}$ current (measured at $V_G=0.8V$, $V_{DS}=0.05V$) and $R_{ON,LIN}$ ($V_G=V_{T,LIN}+0.5V$, $V_{DS}=0.02V$) even if their effect remains relatively limited. For instance, based on our simulations, 90% of dopant deactivation in both extensions and source-drain leads to a current decrease of 43% in sample S1.

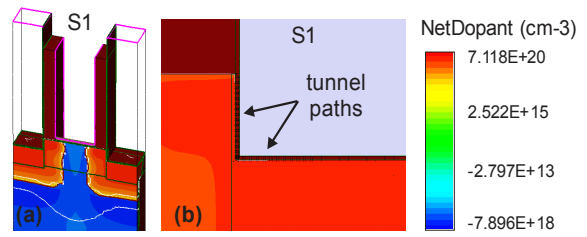


Fig. 9. 3D TCAD dopant map for sample S1 introducing a 0.4nm oxide layer at the LI/epi source-drain interface (a). Zoomed 2D view (b).

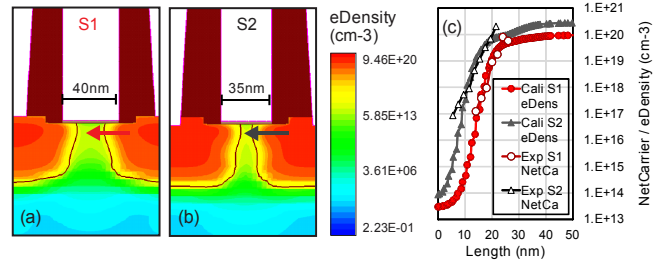


Fig. 10. 2D TCAD carrier maps for samples S1 (a) and S2 (b) after calibration. Arrows are highlighting the lateral section lines from (c). Comparison with quantified 1D sections from s-SSRM (aligned to the gate edge) demonstrate a good agreement between calibrated TCAD and s-SSRM.

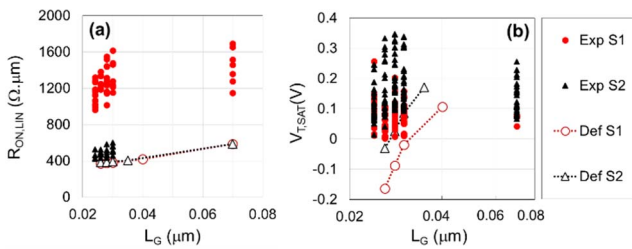


Fig. 7. $R_{ON,LIN}$ as a function of the gate length (L_G) showing the better performance of sample S2 (a). $V_{T,SAT}$ as a function of L_G for samples S1 and S2 exhibiting a more pronounced V_T roll-off in the case of sample S2 (b).

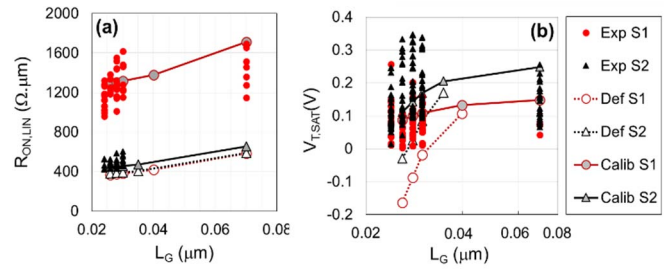


Fig. 11. Simulated versus measured $R_{ON,LIN} - L_G$ (a) exhibiting an improved agreement (mainly as a result of the incorporation in the TCAD simulation of a thin oxide layer at the LI/epi source-drain interface for sample S1). $V_{T,SAT} - L_G$ for samples S1 and S2 (b) exhibiting an improved agreement between simulations and measurements (reduced V_T roll-off in the calibration simulation as compared to default one as a result of the reduced active dose).

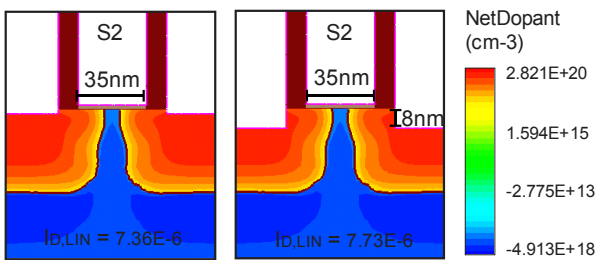


Fig. 8. 2D TCAD dopant maps for sample S2 with default and optimized LI position. The presence of deeper LI contacts is only having a minor impact on the $I_{D,LIN}$.

C. Impact of local interconnects (LI)

We have investigated the impact of the LI depth since experimentally a deeper (8nm) LI (larger recess prior to epi growth) is observed in sample S2. Including this deeper recess in TCAD (Fig. 8) we can however observe that the impact on the $I_{D,LIN}$ current is not large (~5%).

We have also analyzed the impact of the probable presence of a thin oxide layer at the interface between LI and source-drain in sample S1 revealed by a resistance peak in the s-SSRM sections (red circle in Fig.5) and confirmed by energy-dispersive X-ray spectroscopy (EDX) measurements (see in [5]). Introducing a thin (0.4nm) oxide layer at the interface (Fig. 9) is impacting the $I_{D,LIN}$ current significantly (+ 100 %). Note that

such a thin oxide may originate from a not optimized cleaning process prior to the LI silicide formation.

D. Calibration of process simulator and analysis of TCAD results

Taking into account all these indications, we have calibrated our process simulations. For sample S1, corresponding to the implanted source-drain epi, we introduce a dose loss of 90% for the extension and 80% for the epi s/d, with a 0.4nm interfacial oxide. For sample S2, we introduce a dose loss of 50% for the extension and of 66% in the epi s/d. In the optimized 2D TCAD carrier maps as well as the lateral section we obtain a very good agreement with the s-SSRM profiles (Fig. 10). The simulated $V_{T,SAT-LG}$ are in much better agreement with measurements for both samples S1 and S2 (Fig. 11) as the roll-off is reduced (less dopant diffusion into the channel). For sample S2, this also leads to a far better agreement between measured and simulated $R_{ON,LIN-LG}$. For sample S1, however, matching carrier profiles (doss loss) doesn't lead to agreement for $R_{ON,LIN-LG}$ ($I_{D,LIN}$ remains too high). Hence we have to consider the presence of a residual oxide at the contact.

III. PROSPECTIVE WORK AND CONCLUSIONS

Introducing a softer resist strip process at extension and reducing the thermal budget of the epitaxial growth of source-drain, one should be able to further increase the carrier concentration (in particular in the extensions), to reduce the extension overlap and to increase its lateral steepness. Hence roll-off characteristics should be improved and access resistance ($R_{ON,LIN}$) reduced.

The s-SSRM technique has been successfully utilized in order to calibrate process simulations. Impacts of dose loss, thermal budget during epitaxial growth and possible interfacial layers at the LI-epi interface have been highlighted. Tuning these parameters to match the 2D carrier TCAD maps with the s-SSRM maps, we are able to predict more accurately important device parameters and to provide strategy for further improvements in view of the stringent N7 and N5 requirements.

TABLE I. IMPACT OF DOSE LOSS IN EXTENSIONS AND IN SOURCE-DRAIN EPI ON $I_{D,LIN}$ AND $R_{ON,LIN}$ IN S1 AND S2

	Dose	Def S1	Def S2	Ext loss S1	Ext & SD loss S1	Ext & SD loss S2
Ext	1E+14			x	x	
	5E+14					x
S/D	1E+15	x	x			
	3E+14				x	
	1E+15					x
	3E+15	x	x	x		
$I_{D,LIN}$	(μ A)	8.05	7.96	6.90	4.64	6.88
$R_{ON,LIN}$	(Ω,μ m)	360	364	420	625	421

ACKNOWLEDGMENTS

The imec SPM and TEM teams, the TCAD team, the pilot line and amsimec (testlab) are acknowledged for their support.

REFERENCES

- [1] Eyben P, Mody J, Nazir A, Schulze A, Clarysse T, Hantschel T, Vandervorst, "Fundamentals of Picoscience", Ed. CRC Press ISBN 978-1466505094 36 777, 2013.
- [2] L. Zhang et al, "1-nm spatial resolution in carrier profiling of ultrashallow junctions by scanning spreading resistance microscopy", *EEE Electron Device Lett*, 29(7), 799, 2008.
- [3] Eyben P, Clarysse T, Mody J, Nazir A, Schulze A, Hantschel T, and Vandervorst W, "Two-dimensional carrier mapping at the nanometer-scale on 32nm node targeted p-MOSFETs using high vacuum scanning spreading resistance microscopy", *Solid-State Electronics* 71, 69-73, 2012.
- [4] Mody J et al., "3D-carrier Profiling in FinFETs using Scanning Spreading Resistance Microscopy", *IEDM Techn. Digest* 6.1.1-6.1.4, 2011.
- [5] P. Eyben et al., "Scalpel Soft Retrace Scanning Spreading Resistance Microscopy for 3D-carrier profiling in sub-10nm WFIN FinFET", *IEDM Techn. Digest* 14.1.1 - 14.1.4, 2015.